Simulation Modeling of an Enhanced Low-Emission Swirl-Cascade Burner

SEMI-ANNUAL TECHNICAL PROGRESS REPORT

4/01/2003 through 9/30/2003

Dr. Ala Qubbaj, Mechanical Engineering Department

October 2003

DE-FG2602NT41682

University of Texas pan American
1201 West University Drive
Edinburg, Texas 78539-2999

DISCLAIMER NOTICE

This report was prepared as an account of work sponsored by an agency of the United States Government. Neither the United States Government nor any agency thereof, or any of their employees, makes any warranty, express or implied, or assumes any legal liability or responsibility of the accuracy, completeness, or usefulness of any information, apparatus, product, or process disclosed, or represents that its use would not infringe privately owned rights. Reference herein to any specific commercial product, process, or service by trade name, trademark, manufacturer, or otherwise does not necessarily constitute or imply its endorsement, recommendation, or favoring by the United States Government or ant agency thereof. The views and opinions of authors expressed herein do not necessarily states or reflect those of the United States Government or ant agency thereof.

ABSTRACT

The numerical computations were conducted using the *CFD-CHEMKIN* computational program. A cell-centered control volume approach was used, in which the discretized equations or the finite difference equations (FDE) were formulated by evaluating and integrating fluxes across the faces of control volumes in order to satisfy the continuity, momentum, energy and mixture fractions conservation equations. The first order upwind scheme and the well-known SIMPLEC algorithm were used. The standard k-ε model was used to close the set of equations.

The thermal and composition fields in the baseline, cascade, swirl, and swirl-cascade burners were simulated. The temperature and CO_2 concentration fields were just computed and the observations are reported. The analysis of these results is currently underway.

Table of Contents

A. NUMERICAL COMPUTATIONS

A1 Computational Model

Based on the geometric model and boundary conditions applied in the previous phase of the project, the numerical computations were conducted using the *CFD-CHEMKIN* computational program. A cell-centered control volume approach was used, in which the discretized equations or the finite difference equations (FDE) were formulated by evaluating and integrating fluxes across the faces of control volumes in order to satisfy the Favre-averaged continuity, momentum, energy and mixture fractions conservation equations (Eqs. 1, 2, 4 and 9, respectively). The first order upwind scheme was used for evaluating convective fluxes over a control volume. The well-known SIMPLEC algorithm, proposed by Van Dooormal and Raithby[1], was used for velocity pressure-coupling. SIMPLEC stands for "Semi-Implicit Method for Pressure-Linked Equation Consistent", in which an equation for pressure correction is derived from the continuity equation. The standard k-ε model was used to close the set of equations.

A2 Governing Equations

The code CFD-ACE+ employs a conservative finite-volume methodology and accordingly all the governing equations are expressed in a conservative form in which tensor notation is generally employed. The basic governing equations are for the conservation of mass, momentum and energy:

Continuity equation:

$$\frac{\partial \rho}{\partial t} + \frac{\partial}{\partial x_j}(\rho u_j) = 0 \text{ .....} \text{.....(1)}$$

where u_j is the j^{th} Cartesian component of velocity and ρ is the fluid density.

Momentum equations: (j=1, 2, 3)

$$\frac{\partial}{\partial t}(\rho u_j) + \frac{\partial}{\partial x_i}(\rho u_i u_j) = -\frac{\partial p}{\partial x_j} + \frac{\partial \tau_{ij}}{\partial x_i} + \rho f_j \text{ .....(2)}$$

where p is the static pressure, τ_{ij} is the viscous stress tensor and f_j is the body force. For Newtonian fluids τ_{ij} can be expressed as:

$$\tau_{ij} = \mu\left(\frac{\partial u_i}{\partial x_j} + \frac{\partial u_j}{\partial x_i}\right) - \frac{2\mu}{3}\left[\frac{\partial u_k}{\partial x_k}\right]\delta_{ij} \qquad \text{.....(3)}$$

where μ is the fluid dynamic viscosity and δ_{ij} is the Kronecker delta.

Energy Equation:

The equation for the conservation of energy can take several forms. The static enthalpy form of the energy equation can be expressed as:

$$\frac{\partial}{\partial t}(\rho h) + \frac{\partial}{\partial x_j}(\rho u_j h) = -\frac{\partial q_j}{\partial x_j} + \frac{\partial p}{\partial t} + u_j \frac{\partial p}{\partial x_j} + \tau_{ij}\frac{\partial u_i}{\partial x_j} - \frac{\partial}{\partial x_j}(J_{mj} h_m) \text{.....(4)}$$

where J_{mj} is the total (concentration-driven + temperature-driven) diffusive mass flux for species m, h_m represents the enthalpy for species m, and q_j is the j-component of the heat flux. J_{mj}, h_m and h are given as:

$$J_{mj} = -\rho D \frac{\partial Y_m}{\partial X_j} \text{.....(5)}$$

$$h_m = \int_{T_o}^{T} C_{P_m}(T)dT + h_{f_m}^o \text{.....(6)}$$

$$h = \sum_{m=1}^{n} Y_m h_m \text{.....(7)}$$

where D is the diffusion coefficient, C_p is the constant-pressure specific heat, and h_f^o is the enthalpy of formation at standard conditions (P_o=1 atm, T_o=298 K).

The Fourier's law is employed for the heat flux:

$$q_j'' = -K\frac{\partial T}{\partial x_j} \qquad \text{.....(8)}$$

where K is the thermal conductivity.

Mixture Fractions:

$$\frac{\partial}{\partial t}(\rho f_k) + \frac{\partial}{\partial x_j}(\rho u_j f_k) = \frac{\partial}{\partial x_j}\left(D\frac{\partial f_k}{\partial x_j}\right) \text{.....(9)}$$

where D is the diffusion coefficient, f_k is the mixture fraction for the k^{th} mixture.

A3 Chemistry/Reaction Model

The reaction model used by CFD-ACE+ was the instantaneous chemistry model in which the reactants are assumed to react completely upon contact. The reaction rate is infinitely rapid and one reaction step is assumed. Two reactants, which are commonly referred to as “fuel” and “oxidizer”, are involved. A surface “flame sheet” separates the two reactants (this assumption can be made only for nonpremixed flames). The mass fractions for this model are computed by first using Eq. 10 to obtain the composition that would occur without the reaction. The “unreacted” composition, denoted by the superscript “u”, is given by

$$(Y_i)^u = \sum_{k=1}^{K} \xi_{ik} f_k \quad \text{.....(10)}$$

where ξ_{ik} is the mass fraction of the i^{th} species in the k^{th} mixture, Y_i is the mass fraction of the i^{th} species and f_k is the mixture fraction of the k^{th} mixture. The change in composition due to the instantaneous reaction is then added to the unreacted mass fractions, as described below.

A stoichiometrically correct reaction step needs to be specified. The mass of species i produced per unit mass of fuel consumed is

$$r_i = -\frac{\nu_i M_i}{\nu_f M_f} \quad \text{.....(11)}$$

where ν is the stoichiometric coefficient of the species in the overall reaction; positive for product species and negative for fuel and oxidizer. The instantaneous reaction mechanism consumes either all the fuel or all the oxidizer, whichever is limiting. The amount of fuel consumed is

$$\Delta Y_f = \min\left(\frac{(Y_f)^u}{-r_f}, \frac{(Y_{ox})^u}{-r_{ox}}\right) \quad \text{.....(12)}$$

The change in each species due to the reaction is proportional to the change in fuel, with the proportionality constant given by Eq. 11. The mass fraction of each species is then given by

$$Y_i = (Y_i)^u + r_i \Delta Y_f \quad \text{.....(13)}$$

The right-hand side of the above equation is only a function of the K mixture fractions. Therefore, K-1 transport equations were solved for the mixture fractions. These equations have no source terms due to chemical reactions (for more details see Qubbaj[2]).

In this analysis no chemistry model is introduced for the prediction of NO_x formation, and nitrogen is assumed to be chemically inert. NO_x is typically present in very low concentrations in the range of tens to hundreds of parts-per-million (ppm) and therefore has a negligible impact on the major physico-chemical process in combustion. Moreover, NO_x chemistry is orders of magnitude slower compared to the reaction rate of the fuel. NO_x formation is therefore not directly influenced by turbulent mixing; rather it is influenced by mean concentration levels of the primary constituents in the mixture. For this reason, NO_x related computations are typically done in a post-processing phase. Even without a NO_x model, often very useful qualitative information can be gained by studying various aspects of the numerical solution. For example, a high flame temperature and excess amounts of oxygen in the exhaust gases may be indicative of high NO_x emission levels.

B. RESULTS AND DISCUSSION (Partial)

Figure 1 shows the radial temperature profiles for baseline, cascaded, air-swirling, and swirling-cascaded flames in the near burner region, which corresponds to an axial location of x/d=4.63. This near burner region is of primary interest in this study since this is the area where most of the mixing and reactions take place. From the temperature profiles, the following observations can be made: (i) the off-axis peak exists in all cases, however, its radial location moves further inward in the cases of swirl and cascade and outward in the swirl-cascade; (ii) the peak temperature of the air-swirling and cascaded flames drop by 8% and 11%, respectively, from its baseline value, whereas that of the swirl-cascade increases by 8%; (iii) the swirl and cascade profiles are shifted inward towards the fuel-rich side of the flame, whereas the swirl-cascade one is shifted outward; (iv) the air-swirling and cascaded flames have significantly lower temperatures in the fuel-lean side of the flame, compared to the baseline case. However, it has higher valley temperatures in the fuel-rich side. The opposite trend is seen for the swirl-cascade.

Figure 2 depicts the radial concentration profiles of CO_2 at the same conditions pertaining to the earlier temperature profiles. The existence of off-axis peaks, their radial locations, the shift of the profiles, the CO_2 concentrations in the fuel rich and fuel-lean sides, all follow the temperature profiles and similar explanations apply. This is reasonable, since CO_2 is a direct combustion product, which depends primarily on temperature and stoichiometry of the flame.

D. CONCLUSION (pending)

The analysis of the above results is still underway, the conclusions will be made soon

E. REFERENCES

[1]Van doormaal, J. P. and Dryer, F. L., 1984, "Enhancements of the SIMPLE Methods for Predicting Incompressible Fluid Flows," *Numerical Heat Transfer,* Vol. 7, pp. 147-163.

[2]Qubbaj, A. R., 1998, "An Experimental and Numerical Study of Gas Jet Diffusion Flames Enveloped by a Cascade of Venturis," *Ph.D. Dissertation*, School of Aerospace and Mechanical Engineering, The University of Oklahoma, Norman, Oklahoma.

[3]Ala Qubbaj, S. R. Gollahalli and John Villarreal, 2002, "Numerical Modeling of a Turbulent Gas Jet Flame in a Swirling Air Stream," *ASME International Engineering Technology Conference on Energy/Combustion and Alternative Energy Symposium*, February 4-6, Houston, Texas.

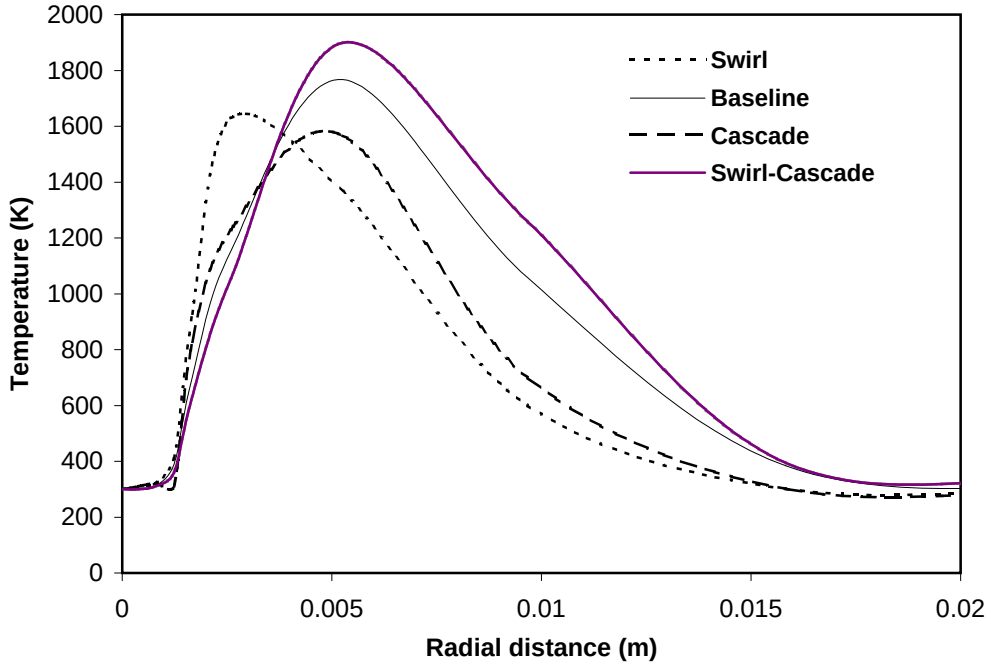

Fig. 1: Temperature Radial Profiles

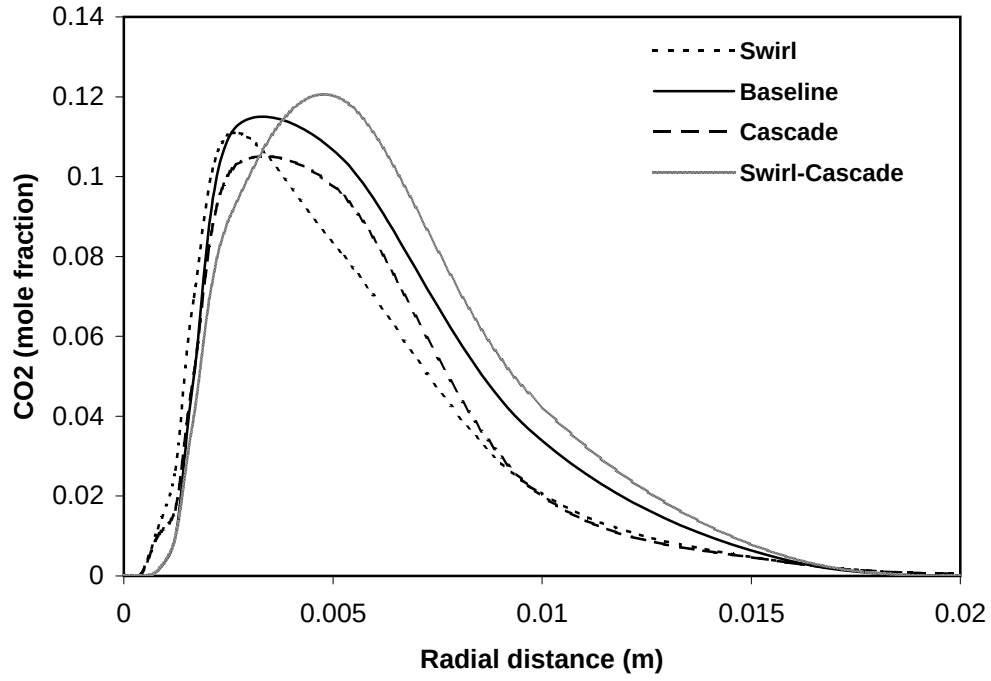

Fig. 2: Carbon Dioxide Radial Profiles